

Dynamical friction in Modified Newtonian Dynamics

Carlo Nipoti¹, Luca Ciotti¹, James Binney², and Pasquale Londrillo³.

¹*Astronomy Department, University of Bologna, via Ranzani 1, 40127 Bologna, Italy*

²*Rudolf Peierls Centre for Theoretical Physics, University of Oxford, 1 Keble Road, Oxford OX1 3NP, UK*

³*INAF-Bologna Astronomical Observatory, via Ranzani 1, 40127 Bologna, Italy*

Accepted 2008 March 3. Received 2008 February 29; in original form 2008 February 8

ABSTRACT

We have tested a previous analytical estimate of the dynamical friction timescale in Modified Newtonian Dynamics (MOND) with fully non-linear N-body simulations. The simulations confirm that the dynamical friction timescale is significantly shorter in MOND than in equivalent Newtonian systems, i.e. systems with the same phase-space distribution of baryons and additional dark matter. An apparent conflict between this result and the long timescales determined for bars to slow and mergers to be completed in previous N-body simulations of MOND systems is explained. The confirmation of the short dynamical-friction timescale in MOND underlines the challenge that the Fornax dwarf spheroidal poses to the viability of MOND.

Key words: gravitation — stellar dynamics — galaxies: kinematics and dynamics

1 INTRODUCTION

Numerous observations indicate that galaxies and clusters of galaxies have gravitational fields that are stronger at large radii than the standard theory of gravity predicts from the conjecture that light is a fair tracer of mass. The standard interpretation of this phenomenon is that $\sim \frac{4}{5}$ of the mass in the Universe is contributed by particles that are dark because they do not interact electromagnetically. The alternative hypothesis, that the standard theory of gravity fails at low accelerations, was advanced by Milgrom (1983). Subsequently Bekenstein & Milgrom (1984) proposed a modification of Poisson’s equation that put the proposal on a quantitative basis. Recently interest in Modified Newtonian Dynamics (MOND) has increased with a growing awareness that relativistically covariant theories are possible that reduce in the non-relativistic limit to the Bekenstein-Milgrom theory (Bekenstein 2004).

One way to rule out MOND would be to detect the particles that are supposed to contribute most of the Universe’s mass, and several experiments are endeavouring to do this under the assumption that the particles have weak interactions. Another way to rule out MOND would be to show that it is inconsistent with observations of the growth of cosmic structure (e.g. Zlosnik et al. 2007) or the dynamics and evolution of galaxies.

In standard gravity, dynamical friction (DF) is thought to play a major role in several astrophysical contexts (e.g. Binney & Tremaine 2008, §8.1). Ciotti & Binney (2004; hereafter CB04) showed that DF is a more potent phenomenon in MOND than in standard gravity, and argued

that it would cause the globular clusters of dwarf spheroidal galaxies to spiral to the centres of their hosts within a dynamical time. However, the results in CB04 were obtained under rather restrictive assumptions and by a non-standard argument that involves the fluctuation-dissipation theorem (see Bekenstein & Maoz 1992). In particular, CB04 gave results for plane-parallel systems that are in the “deep-MOND” regime. Given the prediction of CB04 that DF is much more powerful in MOND than in Newtonian gravity, it is important to test their results with a different approach and in less specialized contexts.

In this paper we use N-body experiments to explore DF in regimes in which departures from Newtonian gravity are of varying magnitude. The paper is organized as follows. In Section 2 we outline our methodology explain our choice of problem. Section 3 gives details of the code and the initial conditions of the simulations. Section 4 presents the results and Section 5 relates them to other recent work. The conclusions and their astronomical implications are summarized in Section 6.

2 METHODOLOGY

Two fundamental features of MOND preclude a direct extension of the standard Chandrasekhar–Spitzer derivation of DF (Chandrasekhar 1942; Spitzer 1987): in MOND (i) forces are not additive and (ii) all two-body orbits are bound, so individual encounters do not have a finite duration. On the other hand, there is no fundamental obstacle to direct simulations of DF in MOND: the drag experienced by a massive

object as it moves through a swarm of less massive objects can be measured in an N-body simulation.

In the classical approach to DF one imagines the background swarm to be homogeneous and perpetrates the Jeans swindle to neglect the mean gravitational field of the swarm. Even in Newtonian gravity this step is of questionable validity, and it is inadmissible in MOND because (i) the long-range nature of two-particle interactions in MOND implies that distant encounters are liable to dominate (in the Newtonian case they nearly do) and (ii) the non-linearity of the Bekenstein–Milgrom field equation implies that the impact of an encounter depends on the nature of the mean field. Therefore, any attempt to extend to MOND the classical approach to DF leads to the consideration of the drag that a massive body experiences as it moves through a self-gravitating system of finite size.

In order to compare the action of DF in MOND and Newtonian systems as cleanly as possible, we compare DF in MOND with DF in the *equivalent Newtonian system* (ENS); that is the Newtonian system in which the visible matter has exactly the same phase-space distribution as in the MOND system (Milgrom 2001; Nipoti et al. 2007b; Nipoti, Londrillo & Ciotti 2007c). In the ENS the visible matter is enveloped in a dark-matter halo that contributes to the DF experienced by a massive body.

There are two astrophysically important problems for which DF is crucial: (i) the inward spiralling of a small system that has fallen into a larger one (e.g. Tremaine, Ostriker & Spitzer 1975; Bontekoe & van Albada 1987; Hernquist & Weinberg 1989; Arena & Bertin 2007), and (ii) the slowing of a massive bar by the material in which it is embedded (e.g. Weinberg 1985; Debattista & Sellwood 1998; Sellwood 2006, and references therein). Our MOND-enabled N-body code (N-MODY; Ciotti, Londrillo & Nipoti 2006; Nipoti, Londrillo & Ciotti 2007a; Londrillo & Nipoti 2008) is better adapted for problem (ii) because it uses a polar grid and therefore has higher resolution at small radii than at large. So we study the effect that MOND has on the rate at which the rotation of a rigid bar is slowed by DF.

3 THE NUMERICAL SIMULATIONS

With Bekenstein & Milgrom (1984) we assume that Poisson’s equation $\nabla^2 \phi^N = 4\pi G\rho$ should be replaced by the non-relativistic field equation

$$\nabla \cdot \left[\mu \left(\frac{\|\nabla\phi\|}{a_0} \right) \nabla\phi \right] = 4\pi G\rho, \quad (1)$$

where $\|\dots\|$ is the standard Euclidean norm, and ϕ is the gravitational potential for MOND; the gravitational acceleration is $\mathbf{g} = -\nabla\phi$ just as the Newtonian acceleration is $\mathbf{g}^N = -\nabla\phi^N$. For a system of finite mass, $\nabla\phi \rightarrow 0$ as $\|\mathbf{x}\| \rightarrow \infty$. The function $\mu(y)$ is constrained by the theory only to the extent that it must run smoothly from $\mu(y) \sim y$ at $y \ll 1$ (the so-called deep-MOND regime) to $\mu(y) \sim 1$ at $y \gg 1$ (the Newtonian regime), with the transition taking place at $y \approx 1$, i.e., when $\|\nabla\phi\|$ is of order the characteristic acceleration $a_0 \simeq 1.2 \times 10^{-10} \text{ m s}^{-2}$. In the present work we adopt $\mu(y) = y/\sqrt{1+y^2}$ (Milgrom 1983).

Table 1. Parameters of the simulations.

Name (1)	Gravity (2)	γ (3)	M_{DM}/M_* (4)	κ (5)	$\Omega_{\text{b},0}/\Omega_*$ (6)	N_{part} (7)
M00	MOND	0	0	1	0.61	8
E00	Newton	0	6.6	1	0.61	16
M01	MOND	0	0	0.1	1.06	8
E01	Newton	0	23.1	0.1	1.06	16
M02	MOND	0	0	0.01	1.88	8
E02	Newton	0	75.3	0.01	1.88	16
M10	MOND	1	0	1	0.74	8
E10	Newton	1	7.0	1	0.74	16
M11	MOND	1	0	0.1	1.27	8
E11	Newton	1	24.4	0.1	1.27	16
M12	MOND	1	0	0.01	2.26	8
E12	Newton	1	79.2	0.01	2.26	16

(1): name of the simulation. (2): gravity law. (3) inner logarithmic slope of the stellar density distribution [equation (2)]. (4): dark matter to baryonic mass ratio. (5): internal acceleration ratio $\kappa \equiv GM_*/(a_0 r_*^2)$. (6): initial angular frequency of the bar, in units of $\Omega_* = 1/t_*$. (7): total number of particles in units of 10^6 .

From Poisson’s equation and equation (1) it follows that the MOND and Newtonian gravitational accelerations are related by $\mu(g/a_0) \mathbf{g} = \mathbf{g}^N + \mathbf{S}$, where $g \equiv \|\mathbf{g}\|$, and \mathbf{S} is a solenoidal field dependent on the specific ρ considered. Since in general $\mathbf{S} \neq 0$, standard Poisson solvers cannot be used to develop MOND N-body codes; equation (1) must be solved at each time step (Brada & Milgrom 1999, Nipoti et al. 2007a).

3.1 The code

N-MODY is a parallel, three-dimensional particle-mesh code that can be used to run either MOND or Newtonian simulations (Nipoti et al. 2007a, Londrillo & Nipoti 2008). In the present study the spherical grid has 128 radial nodes, 64 nodes in colatitude θ and 128 nodes in azimuth ϕ , and the total number of particles is in the range $N_{\text{part}} = 8 \times 10^6 - 1.6 \times 10^7$. We verified with convergence experiments that these numbers of particles and grid points are sufficient to exclude that our results are significantly affected by discreteness effects.

In previous papers (Ciotti, Nipoti & Londrillo 2007, Nipoti et al. 2007ac) we have used N-MODY to demonstrate significant differences in the operation of violent relaxation in systems in which MOND is important and in their Newtonian equivalents. We refer readers to these papers and to Londrillo & Nipoti (2008) for details of the code and its tests.

3.2 Initial conditions

The baryonic component of the initial conditions of the simulations is described by a spherical γ -model (Dehnen 1993; Tremaine et al. 1994) with density distribution

$$\rho_*(r) = \frac{3-\gamma}{4\pi} \frac{M_* r_*}{r^\gamma (r_* + r)^{4-\gamma}}, \quad (2)$$

where M_* is the total stellar mass, r_* is the scale radius, γ is the inner logarithmic slope, and we consider the cases $\gamma = 0$ and $\gamma = 1$ (Hernquist 1990). For a given model, the MOND potential is easily calculated, and to each MOND model with potential ϕ corresponds an ENS with $\phi_{\text{tot}}^{\text{N}} = \phi$, thus having a total density $\rho_{\text{tot}}(r) = \nabla^2 \phi(r)/4\pi G$. In principle, such a distribution would have infinite mass, so we truncate it at $r \sim 10r_*$.

The particles of the stellar component are distributed in phase-space with the standard rejection technique, restricting for simplicity to the fully isotropic case. The MOND distribution function is obtained numerically with an Edington inversion (e.g. Binney & Tremaine 2008, §4.3.1)

$$f_M(E) = \frac{1}{\sqrt{8}\pi^2} \frac{d}{dE} \int_E^\infty \frac{d\rho_*}{d\phi} \frac{d\phi}{\sqrt{\phi - E}}, \quad (3)$$

where the upper integration limit reflects the far-field logarithmic behaviour of the MOND potential.

In the equivalent Newtonian models, at variance with Nipoti et al. (2007c), we do not distinguish between dark and stellar particles, but we consider a single component distributed according to the numerical isotropic distribution function

$$f_N(E) = \frac{1}{\sqrt{8}\pi^2} \frac{d}{dE} \int_E^0 \frac{d\rho_{\text{tot}}}{d\phi_{\text{tot}}^{\text{N}}} \frac{d\phi_{\text{tot}}^{\text{N}}}{\sqrt{\phi_{\text{tot}}^{\text{N}} - E}}. \quad (4)$$

Note that the upper limit of integration is due to the finite mass of the system (a consequence of the density truncation at $10r_*$).

The physical scales of the problem are introduced as follows. First we identify each MOND initial condition by fixing a value for the dimensionless internal acceleration parameter $\kappa \equiv GM_*/(a_0 r_*^2)$, so that M_* and r_* are not independent quantities: in physical units, $r_* \simeq 3.4\kappa^{-1/2} M_{*,10}^{1/2}$ kpc, where $M_{*,10} \equiv M_*/10^{10} M_\odot$. The time and velocity units are $t_* = \sqrt{r_*^3/GM_*} \simeq 29.7\kappa^{-3/4} M_{*,10}^{1/4}$ Myr, and $v_* = r_*/t_* \simeq 112\kappa^{1/4} M_{*,10}^{1/4}$ km s $^{-1}$ (Nipoti et al. 2007a). The simulations are evolved up to $t = 30T_0$ (where T_0 is the initial rotation period of the bar, see Section 3.3), with timestep $\Delta t = 0.003T_0$.

We verified that both the MOND system and its ENS were in equilibrium by running them without the bar for several dynamical times. The dark and luminous matter distributions of the considered ENSs are shown in Fig. 1, plotting, as functions of radius, their dark-matter density $\rho_{\text{dm}} \equiv \rho_{\text{tot}} - \rho_*$ (top panel) and their total (dark-matter plus stars) mass-to-light ratio $M/L \equiv \Upsilon_* \rho_{\text{tot}}/\rho_*$, where Υ_* is the stellar mass-to-light ratio (bottom panel). All the considered ENSs are dark-matter dominated, because the corresponding MOND cases have internal accelerations $\lesssim a_0$. Focusing on the central regions of the ENSs, we note that, for fixed κ , models with cored stellar profile ($\gamma = 0$, dashed curves in Fig. 1) have higher M/L and shallower inner dark-matter profile than models with cuspy stellar profile ($\gamma = 1$, solid curves in Fig. 1). In particular, we have $\gamma_{\text{dm}} \sim 1$ when $\gamma = 1$ and $\gamma_{\text{dm}} \sim 1/2$ when $\gamma = 0$, where $\gamma_{\text{dm}} \equiv -\lim_{r \rightarrow 0} (d \ln \rho_{\text{dm}}/d \ln r)$ is the inner logarithmic slope of the dark-matter density distribution.

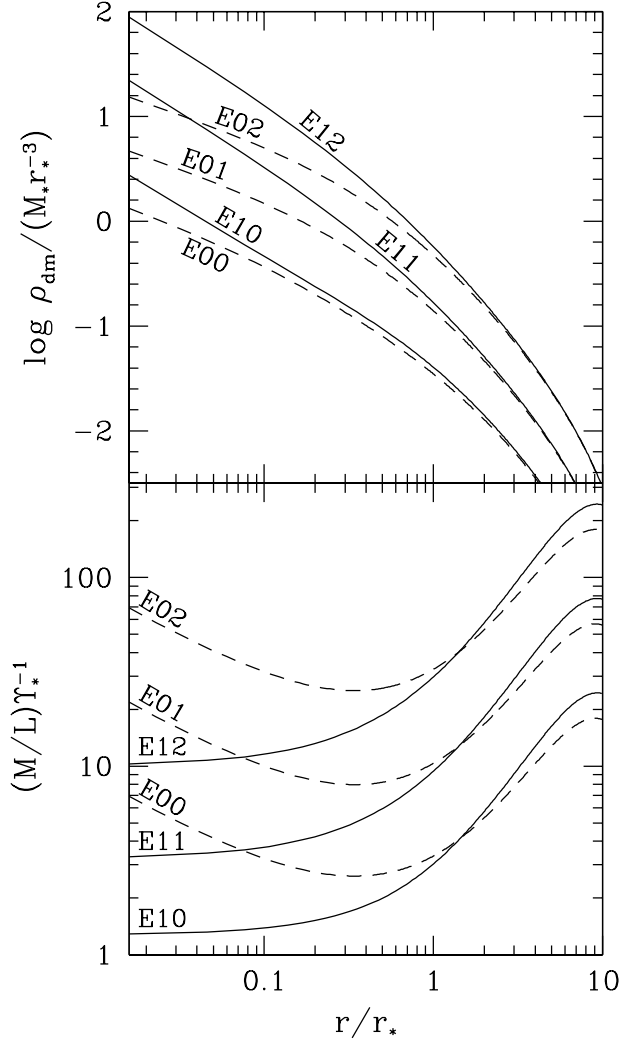


Figure 1. Dark-matter density $\rho_{\text{dm}} \equiv \rho_{\text{tot}} - \rho_*$ (top panel) and total (dark-matter plus stars) mass-to-light ratio M/L (bottom panel) as functions of radius for the equivalent Newtonian models. M/L is in units of the stellar mass-to-light ratio Υ_* . The first digit after “E” is the value of γ while the second digit is $-\log_{10}(\kappa)$ (Table 1). Dashed and solid curves refer to models with $\gamma = 0$ and $\gamma = 1$, respectively.

3.3 Bar equation of motion and the warm-up of the gravitational field

The density distribution of the rigid bar is a prolate ellipsoid of density distribution

$$\rho_b = \frac{M_b}{\pi^{3/2} q b^3} e^{-m^2/b^2}, \quad (5)$$

where in the Cartesian system co-rotating with the bar

$$m^2 = x'^2 + z'^2 + \frac{y'^2}{q^2}, \quad q \geq 1. \quad (6)$$

In all the cases here presented we use $M_b = 0.05M_*$, $b = 0.2r_*$ and $q = 5$: with this choice, the length of the bar’s semi-major axis is r_* . We adopted the distribution (5) because the Gaussian dependence on m produces a bar well defined spatially, but at the same time it avoids a density discontinuity that could produce spurious behaviour in the

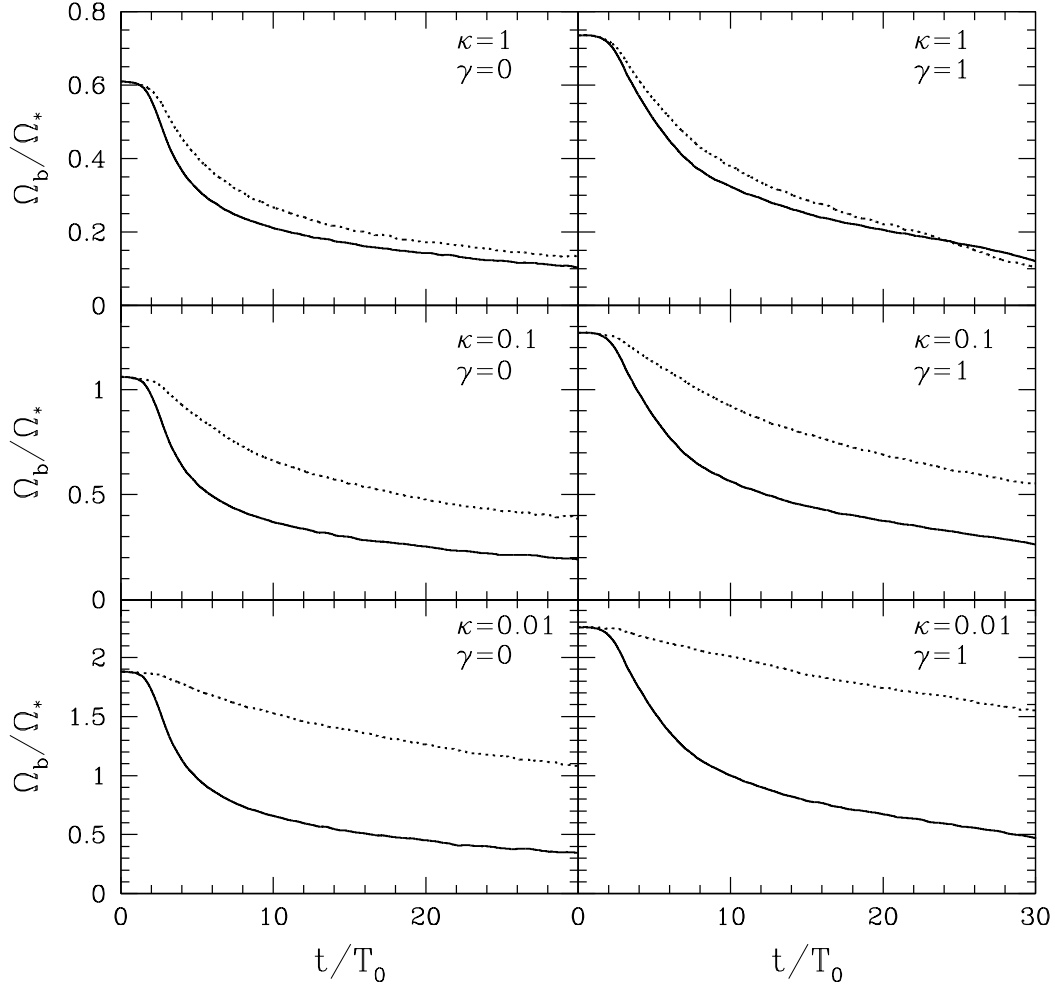


Figure 2. Time evolution of the bar angular frequency in units of $\Omega_* = 1/t_*$ in MOND (solid curves) and equivalent Newtonian models with dark matter (dotted curves), for six pairs of models with different combinations of the parameters κ and γ . Cuspy models are on the right. Smaller values of κ correspond to deeper MOND regimes. Time is normalized to the initial rotation period of the bar T_0 .

potential solver at the bar's edge. In all the simulations the bar rotates around the z' axis.

The Lagrangian formulation can be used to derive the bar's equations of motion in an inertial Cartesian frame (x, y, z) such that $z = z'$: with φ_b the angle in the (x, y) plane between the x and x' axes, we have

$$I_{33} \frac{d^2 \varphi_b}{dt^2} = \int \rho_b(m) \left(y \frac{\partial \phi}{\partial x} - x \frac{\partial \phi}{\partial y} \right) dV, \quad (7)$$

where

$$m^2 = (x \cos \varphi_b + y \sin \varphi_b)^2 + z^2 + \frac{(y \cos \varphi_b - x \sin \varphi_b)^2}{q^2} \quad (8)$$

and from equation (5)

$$I_{33} = \frac{4\pi q(1+q^2)}{3} \int_0^\infty m^4 \rho_b(m) dm = \frac{M_b b^2 (1+q^2)}{2}. \quad (9)$$

In order to start the numerical simulations smoothly, we take the density of the bar to be the product of equation (5) and the function

$$\alpha(t) \equiv \min \left(\frac{t^3}{t_g^3}, 1 \right), \quad (10)$$

where the growth time is $t_g = 3T_0$ with $T_0 \equiv 2\pi/\Omega_{b,0}$ and $\Omega_{b,0}$ is the initial angular velocity of the bar's frame.

As a consequence, when the bar mass is very small, the underlying density distribution is only slightly affected by its gravitational field, and the integral at the r.h.s of equation (7) almost vanishes. Of course, in the MOND simulations, on the r.h.s. of equation (1) we have $\rho = \rho_* + \rho_b$. In all the presented cases we use $\Omega_{b,0} = v_c(r_*)/r_*$, where $v_c(r_*)$ is the circular velocity at r_* (i.e. at the edge of the bar).

For all the simulations, the inner logarithmic slope γ , the internal acceleration ratio κ , the total dark to luminous mass ratio M_{DM}/M_* , the initial angular velocity of the bar $\Omega_{b,0}$ and the total number of particles N_{part} are given in Table 1.

4 RESULTS

CB04 found that the DF timescales in a (deep) MOND system ($t_{\text{fric}}^{\text{M}}$), and in the *equivalent* Newtonian system ($t_{\text{fric}}^{\text{N}}$) are related by

$$\frac{t_{\text{fric}}^{\text{M}}}{t_{\text{fric}}^{\text{N}}} = \frac{\sqrt{2}}{1 + \mathcal{R}}, \quad (11)$$

where $1 + \mathcal{R} \equiv g/g_*$ with g the modulus of the MOND field and g_* the modulus of the Newtonian field *generated by the baryonic distribution*. We recall again that the treatment of CB04 was carried out for a plane-parallel distribution of field particles. In the present case the situation is more complicate, as \mathcal{R} is not constant in the system. Thus, for each pair of simulations with the same value of κ and γ (and therefore with the same gravitational field) we assume as fiducial value $1 + \mathcal{R} = g(r_*)/g_*^{\text{N}}(r_*)$, i.e. we evaluate \mathcal{R} at the edge of the bar. Models with lower values of the parameter κ are in deeper-MOND regime, so \mathcal{R} increases for decreasing κ . In particular, we considered the cases $\kappa = 0.01$, $\kappa = 0.1$ and $\kappa = 1$, so all the models presented have internal accelerations $\lesssim a_0$.

For each simulation, Fig. 2 plots against time the angular frequency of the bar $\Omega_b \equiv \dot{\varphi}_b$; models with constant-density cores are on the left and those with cuspy cores are on the right. Systems with smaller κ and therefore more MOND/dark-matter dominated dynamics are lower down. In each panel the full curve shows the MOND system, and the dotted line its Newtonian equivalent. In every case the bar slows down more in the MOND system than in its ENS.

The instantaneous DF timescale is $|\Omega_b/\dot{\Omega}_b|$, but in practice this quantity fluctuates strongly, so is not a useful measure of the DF timescale. A more robust measure is the time t_{fric} for Ω_b to reach 70% of its initial value, so $\Omega_b(t_{\text{fric}}) = 0.7\Omega_{b,0}$. Figure 3 is a plot against $1 + \mathcal{R}$ of the MOND value of t_{fric} divided by t_{fric} of the ENS. This ratio decreases with κ as predicted by CB04, and in the deep-MOND regime the rate of decrease with increasing $1 + \mathcal{R}$ is consistent with that predicted by CB04 (shown by the full line). The vertical offset between the full line and the points could partly reflect the arbitrariness of our definition of t_{fric} and our assignment of values of \mathcal{R} to simulations. However, we verified that for any sensible definition of \mathcal{R} , the experimental ratio $t_{\text{fric}}^{\text{M}}/t_{\text{fric}}^{\text{N}}$ is always closer to unity than CB04 predicted. Presumably this finding arises because we are considering spherical systems, while CB04 assumed plane-parallel symmetry.

5 RELATION TO OTHER WORK

Tiret & Combes (2007a) used N-body simulations similar, in some respect, to those reported here to compare the dynamics of galactic bars in MOND and in equivalent Newtonian systems. They found that DF had a much *smaller* effect on bars in MOND than in the Newtonian cases. This finding is not in conflict with our opposed finding for this reason: whereas our bars contain only five percent of the galaxy's baryonic mass, in the Tiret & Combes simulations the bars contain the majority of the baryonic mass. Consequently, there is significant background mass for the Tiret & Combes bars to interact with through DF only when dark

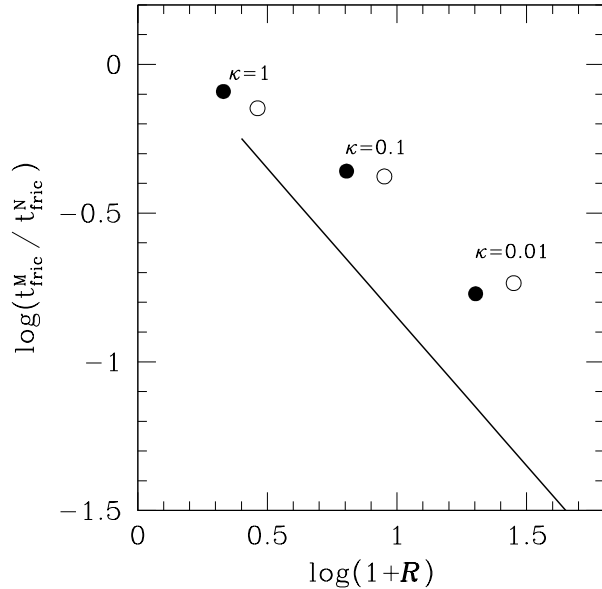


Figure 3. Ratio of MOND and Newtonian equivalent DF timescale t_{fric} as a function of the parameter \mathcal{R} for pairs of models with $\gamma = 1$ (solid symbols) and $\gamma = 0$ (empty symbols). We measure t_{fric} in the simulations as the time for Ω_b to reach 70% of its initial value. The solid line is the ratio as computed by CB04 in the deep-MOND limit.

matter is present. By contrast our bars interact with a background that contains 95 percent of the baryonic mass, so DF is effective.

Similar reasoning applies to the findings of Nipoti et al. (2007c) and Tiret & Combes (2007b) that merging timescales are much longer in MOND than in Newtonian gravity with dark matter: in the Newtonian case there is an abundance of dark matter to absorb energy and angular momentum from the stellar systems, while in MOND the energy and angular momentum has to be absorbed by the outer parts of the stellar systems themselves. Consequently, in the Newtonian case a lot of matter takes up a relatively small amount of energy per particle, and the concept of DF is applicable, while in the case of MOND a small amount of matter takes up a lot of energy per particle, and DF is not an appropriate concept. The prolonged merging timescale in MOND is a consequence of the need to completely transform the orbits of the stars that are absorbing the original orbital energy.

6 CONCLUSIONS

Our fully non-linear simulations of the MOND dynamics of realistic stellar systems nicely confirm the analytical predictions of CB04. In particular, the simulations confirm the predicted scaling of the DF timescale with the parameter $1 + \mathcal{R}$ that measures the extent to which the actual acceleration exceeds that generated by the baryons alone in Newtonian gravity. Consequently, the astrophysical consequences listed in CB04 are confirmed.

Prominent among these was the implication of short

DF timescales for the existence of globular clusters in dwarf spheroidal galaxies. Even simple Newtonian models of dwarf spheroidals and dwarf ellipticals predict that many observed globular clusters should spiral to the galaxy centres within a Hubble time (Tremaine 1976; Lotz et al. 2001). Therefore the existence of objects such as the Fornax dwarf spheroidal, which has five globular clusters but no stellar nucleus that could be the remains of clusters that have spiralled inwards, is a challenge to both Newtonian gravity and MOND. In the context of the standard cold-dark-matter theory, the survival of Fornax's globular cluster against DF is problematic because it can be explained only if the dark matter halo has an extended core, and not a central cusp as predicted by the theory (Goerdt et al. 2006; Sánchez-Salcedo, Reyes-Iturbide & Hernandez 2006). From the point of view of MOND, dwarf spheroidals are in the deep-MOND regime (e.g. Gerhard & Spergel 1992), so the MOND inspiralling time of their globular clusters is as short as the dynamical time. Sánchez-Salcedo et al. (2006) evaluated in detail the predictions of MOND and Newtonian gravity for the fate of the globular clusters of the Fornax dwarf spheroidal galaxy, and from the results of CB04 concluded that Fornax is much more problematic for MOND than for dark matter models. This conclusion gains strength from our confirmation of the central result of CB04.

ACKNOWLEDGEMENTS

We thank Scott Tremaine for useful suggestions, and the anonymous referee for helpful comments. Some of the numerical simulations were performed at CINECA, Bologna, with CPU time assigned under the INAF-CINECA agreement 2007/2008.

REFERENCES

- Arena S.E., Bertin G., 2007, *A&A*, 463, 921
 Bekenstein J., 2004, *Phys. Rev. D*, 70, 3509
 Bekenstein J.D., Maoz E., 1992, *ApJ*, 390, 79
 Bekenstein J.D., Milgrom M., 1984, *ApJ*, 286, 7
 Binney J., Tremaine S., 2008, *Galactic Dynamics* 2nd Ed., Princeton University Press, Princeton
 Bontekoe T.R., van Albada T.S., 1987, *MNRAS*, 224, 349
 Brada R., Milgrom M., 1999, *ApJ*, 519, 590
 Chandrasekhar S., 1942, *Principles of stellar dynamics*, Dover, New York
 Ciotti L., Binney J., 2004, *MNRAS*, 351, 285 (CB04)
 Ciotti L., Londrillo P., Nipoti C., 2006, *ApJ*, 640, 741
 Ciotti L., Nipoti C., Londrillo P., 2007, in Bertin G., Pozzoli R., Romé M., and Sreenivasan K.R., eds., *Collective Phenomena in Macroscopic Systems*, World Scientific, Singapore, p. 177
 Debattista V.P., Sellwood J., 1998, *ApJ*, 493, L5
 Dehnen, W. 1993, *MNRAS*, 265, 250
 Gerhard O.E., Spergel D.N., 1992, *ApJ*, 397, 38
 Goerdt T., Moore B., Read J.I., Stadel J., Zemp M., 2006, *MNRAS*, 368, 1073
 Hernquist L., 1990, *ApJ*, 356, 359
 Hernquist L., Weinberg M., 1989, *MNRAS*, 238, 407
 Milgrom M., 1983, *ApJ*, 270, 365
 Milgrom M., 2001, *MNRAS*, 326, 1261
 Londrillo P., Nipoti C., 2008, *Mem. Soc. Astron. Italiana Supp.*, in press (arXiv:0803.4456)
 Lotz J.M., Telford R., Ferguson H.C., Miller B.W., Stiavelli M., Mack J., 2001, *ApJ*, 552, 572
 Nipoti C., Londrillo P., Ciotti L., 2007a, *ApJ*, 660, 256
 Nipoti C., Londrillo P., Zhao H.S., Ciotti L., 2007b, *MNRAS*, 379, 597
 Nipoti C., Londrillo P., Ciotti L., 2007c, *MNRAS*, 381, L104
 Sánchez-Salcedo F.J., Reyes-Iturbide J., Hernandez X., 2006, *MNRAS*, 370, 1829
 Sellwood J., 2006, *ApJ*, 637, 567
 Spitzer L., (1987) *Dynamical evolution of globular clusters*, Princeton University Press, Princeton
 Tirit O., Combes F., 2007a, *A&A*, 464, 517
 Tirit O., Combes F., 2007b, preprint (arXiv:0712.1459v1)
 Tremaine S.D., 1976, *ApJ*, 203, 345
 Tremaine S.D., Ostriker J.P., Spitzer L., 1975, *ApJ*, 196, 407
 Tremaine, S., Richstone, D.O., Yong-Ik, B., Dressler, A., Faber, S.M., Grillmair, C., Kormendy, J., & Laurer, T.R. 1994, *AJ*, 107, 634
 Weinberg M. D., 1985, *MNRAS*, 213, 451
 Zlosnik T.G., Ferreira P.G., Starkman G.D., 2007, preprint (arXiv:0711.0520v1)